

## Supporting Information for

# Fountain effect of ice-like water across nanotube at room temperature

Kuiwen Zhao and Huiying Wu\*

School of Mechanical Engineering, Shanghai Jiao Tong University, Shanghai, 200240, China.

### Contents

1. Methods.....	2
2. Supporting Figures.....	5
3. Pressure-driven water flow across nanotubes.....	6
4. Velocity profiles of water.....	7
5. Thermodynamics analysis for the fountain effect of water.....	8
6. Power generation by the fountain effect of water.....	9
7. Illustration of Supporting Movie S1.....	12
Reference.....	13

## 1. Methods

All-atom simulations were carried out with LAMMPS <sup>1</sup> using the rigid TIP4P/2005 water model <sup>2</sup>, which precisely predicts the thermodynamic properties for water, including phase diagram, chemical potential, and density <sup>2-3</sup>. The van der Waals parameters for carbon atoms are  $\epsilon_{cc} = 0.07$  kcal mol<sup>-1</sup>, and  $\sigma_{cc} = 3.55$  Å (i.e. sp<sup>2</sup> carbon in the CHARMM27 force field). The cutoff distance for pair interactions is 12 Å. The long-range Coulomb interactions were calculated using Particle-Particle Particle-Mesh (PPPM) method. The size of the simulation systems are 6.2 nm × 6.0 nm × 21.0 nm (Nanotube length  $L = 6.5$  nm) and 6.2 nm × 6.0 nm × 34.5 nm ( $L = 20$  nm), containing 10396 to 11584 water molecules. Periodic boundary conditions were implemented in all directions. Continuous nanotube array membrane is formed by the periodic boundaries. Two pure water reservoirs are separated by this membrane. Empty chambers exist on two sides of the simulation box in  $Z$  direction, avoiding the mixing of cold water and hot water in two water reservoirs. Water molecules with vapor phase move freely across the simulation boundary in  $Z$  direction. In order to avoid any potential spurious physical phenomena caused by thermostats <sup>4-5</sup>, the temperature difference is applied by cooling and heating the water in the pipes (i.e. the blue and red pipes in Fig. 1, Diameter = 2.44 nm) at the bottom and top of the nanotube array, but not cooling and heating the bulk water directly in the simulations. Cooling and heating pipes are 6.0 nm in length and placed along  $Y$ -direction. Water molecules inside and outside the cooling and heating pipes are insulated by the pipes. No water molecule

moves in and out of the pipes. Temperatures of the cooling and heating water in cooling and heating pipes were maintained constant by Langevin thermostats with the damping coefficient  $5 \text{ ps}^{-1}$ . Equations of motion were integrated with a time step of  $2 \text{ fs}$ . Harmonic restraining force ( $1.0 \text{ kcal mol}^{-1} \text{ \AA}^{-2}$ ) was applied to carbon atoms to avoid displacement. Simulation systems were equilibrated at the constant temperature  $((T_H + T_C) / 2)$  and constant pressure (1 bar) before applying a temperature difference. No barostat was applied to the simulation system after applying the temperature difference. Then, before the data collection and analysis, the systems were equilibrated for another 10 ns under the temperature difference generated by the cooling and heating water. No thermostat was applied to the water outside the cooling and heating pipes during this process. The water flow is defined as the net flow of water molecules cross carbon nanotubes from the cold water reservoir to the hot water reservoir, which is numbered with  $\text{molecules} \cdot \text{tube}^{-1} \cdot \text{ns}^{-1}$ . For clarity, water flow velocity numbered with  $\text{m} \cdot \text{s}^{-1}$  is selected to represent the flow strength in the discussion. Here, the water flow velocity is expressed as follows:

$$v = \frac{Flux_m M}{A \rho N_A} \quad (\text{S1})$$

where  $Flux_m$  is the water flux across one nanotube numbered with  $\text{molecules} \cdot \text{tube}^{-1} \cdot \text{ns}^{-1}$ ,  $M$  is the mole mass of water,  $A$  is the cross-section area of nanotube pore ( $0.5275 \text{ nm}^2$  for (15, 0) carbon nanotube),  $\rho$  is the density of water ( $1 \text{ g} \cdot \text{cm}^{-3}$  is selected for simplicity), and  $N_A$  is the Avogadro constant. Thus, we have  $1 \text{ molecules} \cdot \text{tube}^{-1} \cdot \text{ns}^{-1} = 0.0567 \text{ m} \cdot \text{s}^{-1}$ .

To confirm the simulation system is independent of thermostat method, we have tested it with different thermostat methods <sup>4</sup> (Direct rescaling thermostat, Berendsen thermostat, and Langevin thermostat ). Nearly the same directional water flux (26.3 ~ 28.2 molecules·tube<sup>-1</sup>·ns<sup>-1</sup>, Fig. S1) from cold side to hot side is obtained under the same  $T_H$  (365.0 ~ 365.8 K) and  $T_C$  (305.1 ~ 308.0 K).

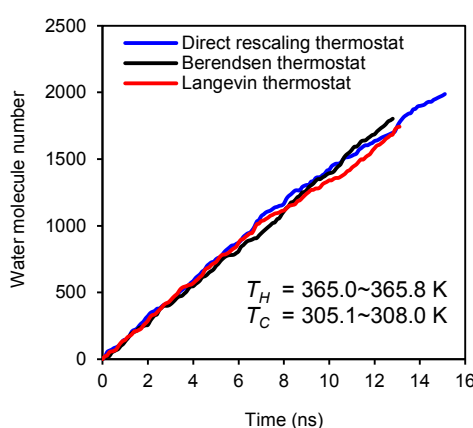


**Figure S1. Net water flow across (15, 0) carbon nanotubes (diameter = 1.17 nm, length  $L = 6.5$  nm, nanotube number  $N = 5$ ) from the cold water reservoir to the hot water reservoir with different thermostats.** Nearly the same directional water flow is observed.

To further confirm the fountain flow is an abnormal phenomenon depending on the ice-like ordered water inside nanotubes, we have simulated the water flow across (15, 15) carbon nanotubes (diameter = 2.03 nm) under  $T_H = 365.5$  K and  $T_C = 309.4$  K (no ice-like ordered water is observed inside the nanotubes during this process), no obvious directional water flow is observed (Fig. S2a). The small bidirectional flow is caused by the bidirectional diffusion of water across nanotubes induced by thermal fluctuation (Fig. S2b).). We can infer that the fountain effect cannot occur for water across

nanotubes with the diameter above 2 nm because the ice-like ordered water cannot appear inside the nanotubes at  $T > 273.15$  K and  $P = 1$  atm<sup>6-7</sup>.

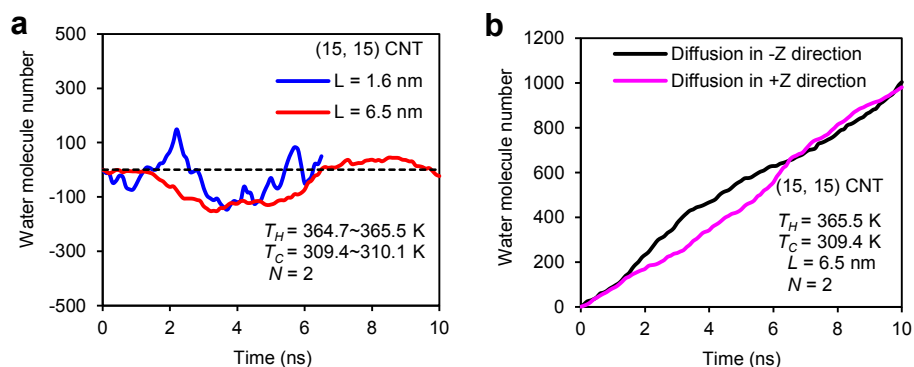


**Figure S2.** (a) Net water flow across (15, 15) carbon nanotubes (diameter = 2.03 nm,  $L = 1.5$  nm, 6.5 nm,  $N = 2$ ) under a temperature difference. No directional water flow is observed. (b) Bidirectional diffusion of water molecules across nanotubes induced by thermal fluctuation

## 2. Supporting Figures

### Supporting Figure S3

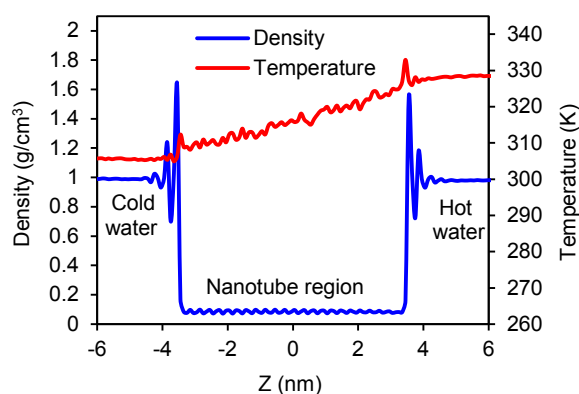


**Figure S3. Temperature and density of water along nanotube axis.** The size of analysis slices is 0.1 nm in Z direction, 2 nm in X direction, and 3 nm in Y direction. The data is averaged over 18 ns. The density of water in two water reservoirs corresponds well to the density of water at 1 bar under the same temperature (deviation  $< 0.46\%$ ).<sup>2</sup>

## Supporting Figure S4

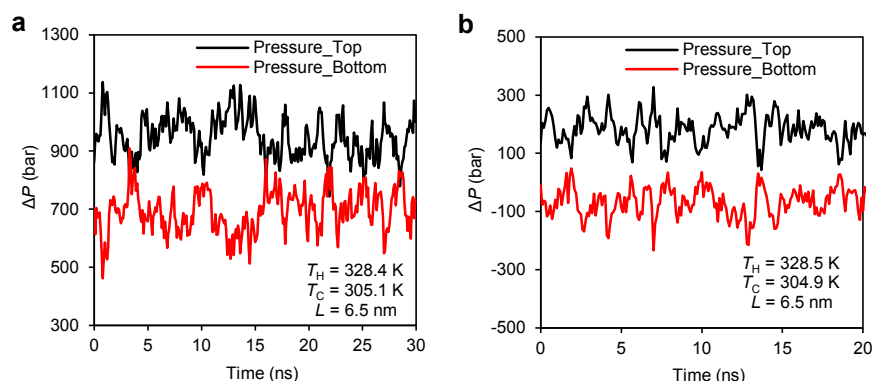


**Figure S4. Pressure acting on graphene sheets on the top and bottom of simulation system by water.** To confirm the fountain effect is independent of pressure, we have take a additional test (Fig. S4b) under the same  $T_H$  and  $T_C$  at low pressure. Nearly the same pressure difference is obtained (250.5 bar).

### 3. Pressure-driven water flow across nanotubes

To evaluate the power strength of the fountain effect of water, we determine water flux under various pressure difference as a comparison. A pressure difference of 250, 500 bar in axial direction of nanotubes is generated by applying a force in axial direction on water molecules (Fig. S5a)<sup>8</sup>. The water flux is proportional to the pressure difference (Fig. S5b), which is consistent to the water flux under the same pressure difference induced by the fountain effect of water (Fig. 1d).

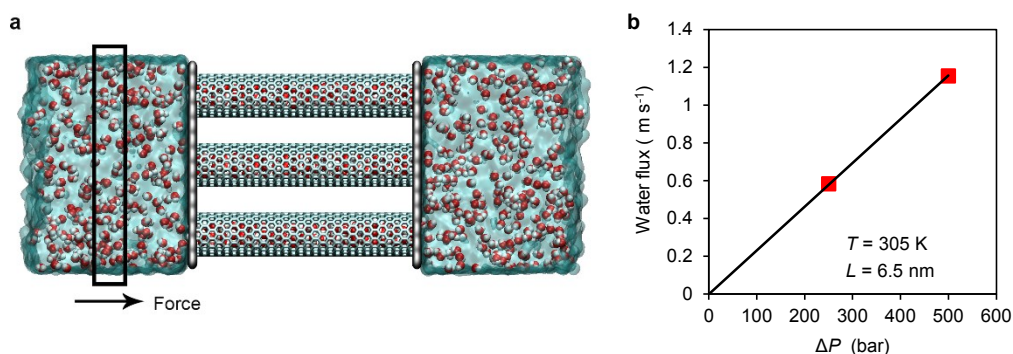


**Figure S5. Pressure-driven water flow across nanotubes.** **a**, Molecular system to determine water flux across nanotubes under a pressure difference. A constant force in axial direction is applied on water molecules within the black box, generating a pressure difference between two water reservoirs. **b**, Water flux across nanotubes as a function of pressure difference. Two water reservoirs are maintained at the same temperature (305 K).

#### 4. Velocity profiles of water

During the fountain flow process, all water molecules in nanotubes move in the same direction, no radial diffusion and axial diffusion are observed. All water molecules maintain ballistic transport (Supporting Movie S1) and show the same velocity profile in axial direction (Fig. S6).

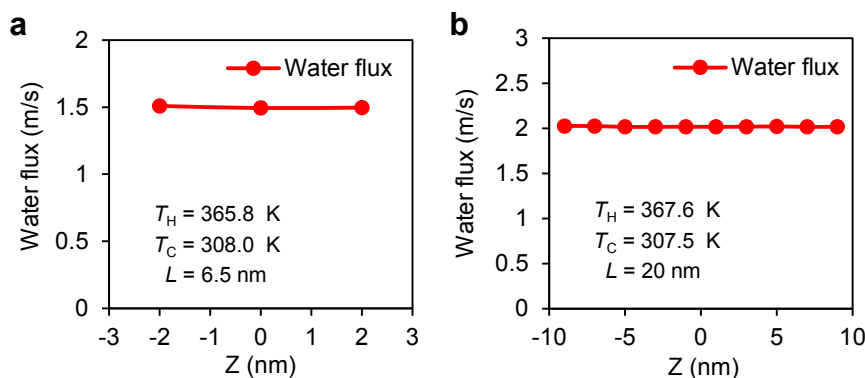


**Figure S6. Velocity profiles for water in axial direction.**

The water molecules in nanotubes maintain pentagonal ordered ring-like structures (Fig. S7a). Water molecules hydrogen bond with each other in the ring-like structure and stack together to form a solid-like highly ordered water structure (Fig. S7b). All water molecules move in the same direction (flow direction). Accordingly, no water flow observed in radial direction.

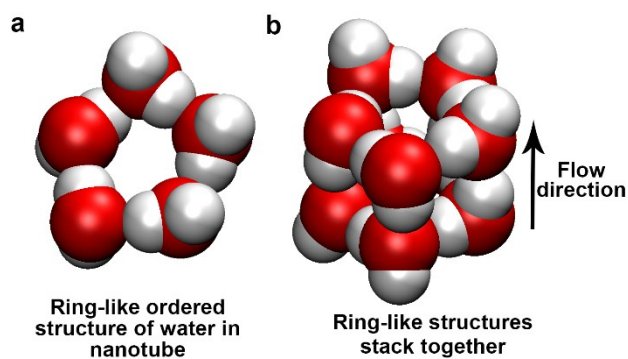


**Figure S7.** Molecular arrangement of water molecules with ice-like ordered structures

## 5. Thermodynamics analysis for the fountain effect of water

According to the second law of thermodynamics, the total entropy of the system and environment does not decrease during the fountain flow process, which can be simply expressed as:

$$\frac{Q_C}{T_C} - \frac{Q_C + w_m + Q_{water}}{T_H} + \Delta S_{water} \geq 0 \quad (\text{S2})$$

where  $Q_C$  is the heat release as water molecules move from cold water reservoir into nanotubes (456 J g<sup>-1</sup> at 305 K, determined by enthalpy change between two water phases with molecular dynamics simulations),  $w_m$  is the maximum mechanical work output,  $Q_{water}$  and  $\Delta S_{water}$  are the heat absorption and entropy change, respectively, for water changing from the cold temperature  $T_C$  at low pressure  $P_C$  to the hot temperature

$T_H$  at high pressure  $P_H$ .

Equation S2 can be written as

$$\Delta S_{water} - \frac{Q_{water}}{T_H} + \frac{Q_C}{T_C} - \frac{Q_C + w_m}{T_H} \geq 0 \quad (S3)$$

In this work,  $\Delta S_{water} - \frac{Q_{water}}{T_H} > 0$ . Thus, Equation S3 is absolutely tenable when:

$$\frac{Q_C}{T_C} - \frac{Q_C + w_m}{T_H} \geq 0 \quad (S4)$$

Substituting  $w_m = \Delta P / \rho_{T_H}$  into Equation S4, we obtain:

$$\frac{Q_C}{T_C} - \frac{Q_C + \Delta P / \rho_{T_H}}{T_H} \geq 0 \quad (S5)$$

Substituting  $\Delta T = T_H - T_C$  into Equation S5, we obtain:

$$\frac{\Delta P}{\Delta T} \leq \frac{Q_C}{T_C} \rho_{T_H} = S_{T_C} \rho_{T_H} \quad (S6)$$

where  $S_{T_C}$  is the entropy change for the transition between free bulk water in cold reservoir to ordered water structure inside nanotubes, and  $\rho_{T_H}$  is the density of bulk water at the temperature of  $T_H$ . Heat release  $Q_C$  is 456 J g<sup>-1</sup> at 305 K, and water density is about  $1 \times 10^6$  g m<sup>-3</sup>. Thus

$$\frac{\Delta P}{\Delta T} \leq \frac{Q_C}{T_C} \rho_{T_H} = \frac{456 \text{ J g}^{-1}}{305 \text{ K}} \times 1 \times 10^6 \text{ g m}^{-3} = 1.50 \times 10^6 \text{ Pa K}^{-1} = 15.0 \text{ bar K}^{-1} \quad (S7)$$

## 6. Power generation by the fountain effect of water

Considering the water flux across nanotubes is proportional to the pressure difference (Fig. S4b), mechanical work output per unit time  $w$  by fountain flow across one nanotube can be determined by:

$$w = P_{Driving} \frac{Flux}{\rho} = P_{Driving} \frac{\Delta P - P_{Driving} F_{Max}}{\Delta P} \frac{F_{Max}}{\rho} \quad (S8)$$

where  $P_{Driving}$  and  $Flux$  are the driving pressure and mass flux of water across one nanotube under the driving pressure, respectively.  $\rho$  is the water density at  $T_H$ .  $\Delta P$  and  $F_{Max}$  are the maximum pressure difference and mass flux of water across one nanotube, respectively, induced by the fountain effect of water.

Here we consider an a nanotube array with  $N = 1.5 \times 10^{13}$  nanotubes per square centimeter<sup>9</sup>. Then the power density is  $W = Nw$ .

Schematic diagram of energy transport during the fountain effect process is shown in Fig. S8. Phase change occurs as water move into nanotubes and a large amount of heat ( $Q_C$ ) is released to the cold water reservoir during this process. On the other hand, a large amount of heat ( $Q_A$ ) is absorbed from the hot water reservoir as water move out of nanotubes and change from ice-like ordered structure to free liquid phase. The mechanical work output per unit time ( $w$ ) comes from the difference between heat absorption and release. Besides, thermal energy is lost to environment through heat transfer across nanotube ( $Q_{Loss}$ ). When water flows from cold water reservoir to hot water reservoir, thermal energy is absorbed by water ( $Q_{water}$ ) from hot source to change

from the cold temperature  $T_C$  at low pressure  $P_C$  to the hot temperature  $T_H$  at high pressure  $P_H$ , which is inevitable consumption. Thus, the overall energy consumption per unit time can be expressed as:

$$E_C = Q_H Flux = (Q_A + Q_{water} + Q_{Loss}) Flux \quad (S9)$$

Part of the thermal energy  $Q_A$  is converted into mechanical work. The rest ( $Q_C$ ) is released to the cold water reservoir. Thus the heat absorption  $Q_A$  per unit time can be expressed as:

$$Q_A Flux = Q_C Flux + w \quad (S10)$$

Substituting Equation S10 into Equation S9, we obtain:

$$E_C = Q_H Flux = (Q_C + Q_{water} + Q_{Loss}) Flux + w \quad (S11)$$

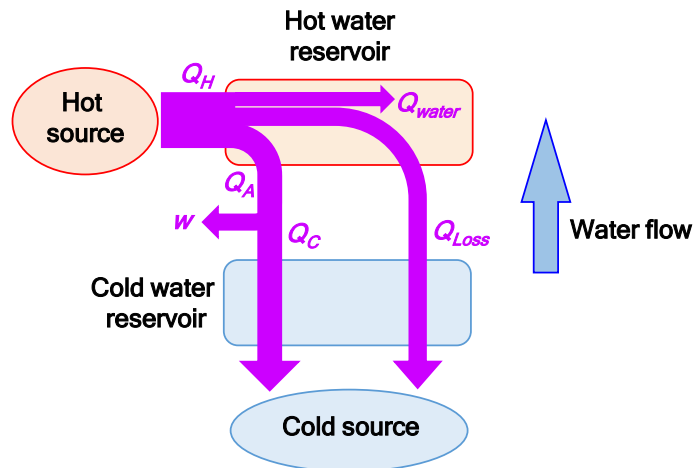


**Figure S8.** Schematic diagram of energy transport during the fountain effect process.

Here  $Q_H$  is total thermal energy consumption,  $Q_A$  is the heat absorption as water molecules move from nanotube into hot water reservoir,  $Q_C$  is the heat release as water

molecules move from cold water reservoir into the nanotube,  $w$  is the mechanical work output per unit time,  $Q_{water}$  is the heat absorption for water changing from the cold temperature  $T_C$  at low pressure  $P_C$  to the hot temperature  $T_H$  at high pressure  $P_H$ , and  $Q_{Loss}$  is the heat loss through heat transfer across the nanotube.

The energy conversion efficiency  $\eta$  is the ratio of the mechanical work output to the total thermal energy consumption, determined by:

$$\eta = \frac{w}{Q_H Flux} = \frac{w}{(Q_C + Q_{water} + Q_{Loss}) Flux + w} \quad (S12)$$

where,  $w$  is determined by Equation S6, and  $Q_C$  is determined by enthalpy difference between ice-like ordered water inside nanotubes and free liquid water in cold water reservoir with molecular dynamics simulations (456 J g<sup>-1</sup> at 305 K). The heat loss through heat transfer across one nanotube  $Q_{Loss}$  can be simply determined by:<sup>10-11</sup>

$$Q_{Loss} = \frac{\Delta T}{\frac{L}{kA} + \frac{2}{hA}} \quad (S13)$$

where  $\Delta T$  is the temperature difference between water reservoirs,  $L$  is the nanotube length,  $k$  is the thermal conductivity of carbon nanotubes ( $\sim 3500$  W m<sup>-1</sup> K<sup>-1</sup> <sup>11-12</sup>),  $h$  is the interface thermal conductance of water-carbon interfaces ( $7.2 \times 10^5$  W m<sup>-2</sup> K<sup>-1</sup> <sup>13</sup>), and  $A$  is the cross-sectional area of the nanotube (1.25 nm<sup>2</sup> for (15,0) carbon nanotube). As stated by the reference <sup>6</sup>, the axial thermal conductivity of carbon nanotubes filled with water is substantially reduced by 500%. According to Equation S10, the heat loss across nanotube decreases no more than 0.1% for nanotube with  $L = 6.5$  nm as the thermal conductivity of nanotubes is reduced from 3500 W m<sup>-1</sup> K<sup>-1</sup> to 700 W m<sup>-1</sup> K<sup>-1</sup>.

The heat loss decreases 27% for long nanotube ( $L = 1 \text{ mm}$ ). By contrast, the reduction of interface thermal conductance is more effective to decrease the heat loss. The heat loss decreases 50% if the interface thermal conductance is reduced by 50% ( $L = 6.5 \text{ nm}$ ).

## 7. Illustration of Supporting Movie S1

All water molecules in nanotubes maintain ballistic transport behavior and no radial or axial diffusion induced by thermal fluctuation exists. For clarity, fifteen water molecules are shown with red (O) and white (H) spheres to track the motion trajectory of water molecules.

### Reference

1. Plimpton, S. Fast parallel algorithms for short-range molecular dynamics. *J. Comput. Phys.* **1995**, *117* (1), 1-19.
2. Abascal, J. L. F.; Vega, C. A general purpose model for the condensed phases of water: TIP4P/2005. *J. Chem. Phys.* **2005**, *123* (23), 234505.
3. Guse, C.; Hentschke, R. Simulation Study of Structural, Transport, and Thermodynamic Properties of TIP4P/2005 Water in Single-Walled Carbon Nanotubes. *J. Phys. Chem. B* **2012**, *116* (2), 751-762.
4. Thomas, M.; Corry, B. Thermostat choice significantly influences water flow rates in molecular dynamics studies of carbon nanotubes. *Microfluidics and Nanofluidics* **2015**, *18* (1), 41-47.

5. Page, A. J.; Isomoto, T.; Knaup, J. M.; Irle, S.; Morokuma, K. Effects of Molecular Dynamics Thermostats on Descriptions of Chemical Nonequilibrium. *J. Chem. Theory Comput.* **2012**, *8* (11), 4019-4028.
6. Agrawal, K. V.; Shimizu, S.; Draushuk, L. W.; Kilcoyne, D.; Strano, M. S. Observation of extreme phase transition temperatures of water confined inside isolated carbon nanotubes. *Nat. Nanotechnol.* **2017**, *12* (3), 267-273.
7. Zhao, K.; Wu, H. Structure-dependent water transport across nanopores of carbon nanotubes: toward selective gating upon temperature regulation. *Physical Chemistry Chemical Physics* **2015**, *17* (16), 10343-10347.
8. Zhu, F.; Tajkhorshid, E.; Schulten, K. Pressure-Induced Water Transport in Membrane Channels Studied by Molecular Dynamics. *Biophys. J.* **2002**, *83* (1), 154-160.
9. Zhong, G.; Warner, J. H.; Fouquet, M.; Robertson, A. W.; Chen, B.; Robertson, J. Growth of Ultrahigh Density Single-Walled Carbon Nanotube Forests by Improved Catalyst Design. *ACS Nano* **2012**, *6* (4), 2893-2903.
10. Incropera, F. P. *Fundamentals of Heat and Mass Transfer*. John Wiley & Sons: 2011.
11. Marconnet, A. M.; Panzer, M. A.; Goodson, K. E. Thermal Conduction Phenomena in Carbon Nanotubes and Related Nanostructured Materials. *Rev. Mod. Phys.* **2013**, *85* (3), 1295-1326.
12. Pettes, M. T.; Shi, L. Thermal and Structural Characterizations of Individual Single-, Double-, and Multi-Walled Carbon Nanotubes. *Adv. Funct. Mater.* **2009**, *19*

(24), 3918-3925.

13. Hong, T.; Cao, Y.; Ying, D.; Xu, Y.-Q. Thermal and Optical Properties of Freestanding Flat and Stacked Single-layer Graphene in Aqueous Media. *Appl. Phys. Lett.* **2014**, *104* (22), 223102.